Beads Based Electrochemical Assay for Detection of Hemagglutinin Labeled by Two Different Types of Cadmium Quantum Dots

Ludmila Krejcova[1], David Hynek[1,2], Roman Guran[1,2], Petr Michalek[1,2], Amitava Moulick[1,2], Pavel Kopel[1,2], Katerina Tmejova[1,2], Nguien Viet Hoai[1,2], Vojtech Adam[1,2], Jaromir Hubalek[1,2], Jindrich Kynicky[3], Rene Kizek[1,2]*

[1] Department of Chemistry and Biochemistry, Faculty of Agronomy, Mendel University in Brno, Zemedelska 1, CZ-613 00 Brno, Czech Republic, European Union
[2] Central European Institute of Technology, Brno University of Technology, Technicka 3058/10, CZ-616 00 Brno, Czech Republic, European Union
[3]Karel Englis College, Sujanovo nam. 356/1, CZ-602 00, Brno, Czech Republic, European Union
*E-mail: kizek@sci.muni.cz

In this study it is described beads based isolation assay terminated by electrochemical analysis of hemagglutinin (HA) using two different cadmium quantum dots (QDs) labelled as CdS and CdTe. The two steps assay was suggested as the first step was the automatic isolation of HA labelled by Cd QDs using glycan modified paramagnetic particles (MPs), and the second one was the electrochemical detection of HA-QDs complex by voltammetry, particularly, adsorptive transfer technique coupled with differential pulse voltammetry Brdicka reaction was used for detection of HA and differential pulse anodic stripping voltammetry was used for detection of Cd. Both methods were optimized. Suggested assay can be used for the subtyping and quantification of HA.

1. INTRODUCTION

One of the great treat of humanity across the history is pandemic occurrence. 21st century, which is marked by increasing globalization, airplane transport together with population growth, multiplies this risk [1]. Influenza belongs to the most dangerous due to high rateof mutation of surface´s influenza antigens as hemagglutinin (HA) and neuraminidase (NA) [2]. Influenza viruses are pathogens capable of continuously evading immune response. Accumulation of mutations in the

antigenic sites is called the "antigenic drift" [3,4]. In circulating influenza viruses this antigenic drift is a major process, which accumulates mutations of the antibody binding sites of receptor proteins and enables the virus to evade recognition by hosts' antibodies, which often translates into periodic epidemics of influenza [3,5]. HA and NA play opposite roles in interaction of virus with host cell receptor [6]. HA initiates the infection and binds sialic acid receptor. NA eliminates sialic acid from host cell receptor, which HA bound and allows the release of new replicated virions [7]. There have been identified 9 subtypes of NA (1-9) and 16 subtypes of HA (1-16). All known subtypes (HxNy) are found in birds, but many subtypes are endemic in humans, cats, dogs, horses, ferrets and wheals [8-10]. There are several experts that believe that only influenza A viruses of the A/H1, A/H2, and A/H3 subtypes can cause pandemics, as no other virus subtypes are known to cause pandemics in the past [11]. There were three great pandemic in the last century. The first one „Spanish flu" (H1N1, 1918), which was considered as the biggest one with 50 million victims [12], and it was followed by two others, but moderate pandemics: Asian Flu (H2N2, 1957) and Hong-Kong flu (H3N2, 1968) [13]. However, based on historical records, most influenza experts agree with one thing that there will likely be future pandemics, of unknown severity [14,15]. The influenza A virus that will most probably cause the next influenza pandemic is a highly debated topic in virology [16]. To the influenza spread, a flexible vaccination WHO's program, based on periodic production of novel versions of vaccine, is adapted to the actually prevalent stain(s) [3]. HA is considered to be the main target for antibodies upon vaccination or native infection and is the key component of the vaccine. Quantitative and qualitative analysis of HA is crucial-point before the vaccine is placed to the market. Therefore, suitable tools for this purpose are still searched for.

Separation of magnetic-bead-labelled biomolecules (or cells) from a liquid solution is well documented and widely practiced application today and is extremely important in process engineering [17]. Paramagnetic particles (MPs) are considered as the unique isolation tool with broad spectrum of features (easy handling by the magnet, well modified surfaces and large surface to small size) [18,19]. In this study we used streptavidin modified MPs for binding biotinylated glycan due to streptavidin-biotin affinity. This step was followed by linkage of Cd QDs labelled vaccine hemagglutinin to glycan modified MPs. End point of isolation was electrochemical analysis of both HA-QDs complexes. Two different techniques of differential pulse voltammetry (DPV) were used.

2. EXPERIMENTAL PART

2.1. Chemicals

Tris(2-carboxyethyl)phosphine (TCEP) was from Molecular Probes (Oregon, USA). $Co(NH_3)_6Cl_3$ and other chemicals were purchased in ACS purity from Sigma Aldrich (Sigma-Aldrich, USA) unless indicated otherwise. Stock solutions were prepared with ACS water. pH value was measured using inoLab Level 3 (Wissenschaftlich-Technische Werkstatten GmbH; Weilheim, Germany). Deionised water underwent demineralization by reverse osmosis using Aqua Osmotic 02 (Aqua Osmotic, Tisnov, Czech Republic) and was subsequently purified using Millipore RG (MiliQ

water, 18 MΩ, Millipore Corp., USA). Deionised water was used for rinsing, washing and preparation of buffers.

2.2. Hemagglutinin

As the standards of HA of Influenza A and B types, influenza vaccine Vaxigrip® (Sanofi Pasteur, France), which contains inactivated and split virions of the following strands: A/California/7/2009 (H1N1)-derived strain used NYMC X-179A, A/Perth/16/2009 (H3N2)-like strain used NYMC X-187 derived from A/Victoria/210/2009 and B/Brisbane/60/2008, was used. Strains were propagated in fertilised hens 'eggs from healthy chicken flocks. Vaxigrip® contains 15 micrograms of all of three HA per 0.5 ml.

2.3. Quantum dots

2.3.1. Preparation of CdS quantum dots

CdS quantum dots (QDs) were prepared using a slightly modified version of the published method [20]. Cadmium nitrate tetrahydrate $Cd(NO_3)_2 \cdot 4H_2O$ (0.1 mM) was dissolved in ACS water (25 ml). 3-mercaptopropionic acid (35 µl, 0.4 mM) was slowly added to the stirred solution. Afterwards, the pH was adjusted to 9.11 with 1 M NH_3 (1.5 ml). Sodium sulphide monohydrate $Na_2S \cdot 9H_2O$ (0.1 mM) in ACS water was poured into the solution while vigorously stirring. The acquired yellow solution was stirred for 1 h. Prepared CdS-quantum dots were stored in the dark at 4 ºC.

2.3.2. Preparation of CdTe quantum dots

CdTe QDs were prepared according to slightly modified method published by *Duan et al.* [21]. Briefly, cadmium acetate dihydrate $Cd(OAc)_2 \cdot 2H_2O$ (0.0267 g) was dissolved in ACS water (44 ml) and 100 mg of trisodium citrate dihydrate was added with stirring. Solution of 0.0055 g Na_2TeO_3 in 1.25 ml of water was poured into the first solution followed by 3-mercaptopropionic acid (100 µl, 1.14 mM). Afterwards, solid $NaBH_4$ (50 mg) was added with vigorous stirring and hydrogen evolution was observed, followed by colour change of solution to slightly yellow. After 30 min of stirring, 2 ml of solution was heated in glass vial in Multiwave 3000 Microwave Reaction System (Anton Paar, Graz, Austria) using rotor 64MG5. Reaction conditions were as it follows: power 300 W, 120 ºC and time 18 min. Obtained CdTe QDs were stored in dark at 4 ºC.

2.4. Labelling of HA from Vaxigrip by QDs

Vaxigrip® (500 µl containing of 45 µg HA) was reduced and washed with water (5 x 400 µl) on an Amicon 3k centrifugal filter device (Millipore, Massachusetts, USA) and mixed with a solution of prepared QDs (500 µl). This mixture was shaken for 24 h at room temperature (Biosan Orbital

Shaker OS-10, Biosan Ltd. Riga, Latvia). The volume of solution was reduced to 100 µl on an Amicon Ultra 3k, diluted with water and washed 5 times using centrifuge 5417R (Eppendorf, Hamburg, Germany). The washed sample was diluted to 1 ml with ACS water and used for measurements.

2.5. Characterization of vaxi HA, CdTe and CdS, HA-CdS and HA-CdTe complex by electrochemical analysis

2.5.1. Characterization of hemagglutinin by AdT DPV

Characterization of HA and its complex with quantum dots by adsorptive transfer technique coupled with differential pulse voltammetry (AdT DPV) were performed with a 663 VA Stand instrument (Metrohm, Herisau, Switzerland), which was equipped with a standard cell consisting of three electrodes, a cooled sample holder and a measurement cell set at 4 °C (Julabo F25, JulaboDE, Seelbach, Germany). The three-electrode system was consisted of a hanging mercury drop electrode (HMDE) with a drop area of 0.4 mm^2 as the working electrode, an Ag/AgCl/3M KCl reference electrode and a platinum electrode acting as the auxiliary. Software GPES 4.9 was used for data analysis. The analysed samples were deoxygenated prior to measurement by purging with argon (99.999 %) saturated with water for 120 s. Brdicka supporting electrolyte containing 1 mM $Co(NH_3)_6Cl_3$ and 1M ammonia buffer ($NH_3(aq) + NH_4Cl$, pH = 9.6) was used. The supporting electrolyte was exchanged after each analysis. The parameters of the measurement were as follows: initial potential of -0.7 V; end potential of -1.75 V; modulation time 0.057 s; time interval 0.2 s; step potential 0.002 V; modulation amplitude 0.025V sample volume: 5 µl. Time of accumulation was optimized.

2.5.2. Detection of cadmium by DPASV

Cd in QDs itself and Cd from HA-QDs complexes were detected by differential pulse anodic stripping voltammetry (DPASV). All of measurements were performed using a 663 VA Stand (Metrohm), equipped with a standard cell with three electrodes. The three electrode system was consists of a hanging mercury drop electrode (HMDE) with a drop area of 0.4 mm^2 as the working electrode, an Ag/AgCl/3M KCl reference electrode and a glassy carbon acting as the auxiliary electrode. GPES 4.9 software was employed for data processing. The analysed samples were deoxygenated prior to measurements by purging with argon (99.999%). Acetate buffer (0.2 M $CH_3COONa + CH_3COOH$, pH 5) was used as a supporting electrolyte. The supporting electrolyte was replaced after each analysis. The parameters of the measurement were as follows: purging time 100 s; deposition potential -0.85 V; equilibration time 2 s; modulation time 0.057 s; interval time 0.2 s; initial potential -0.85 V; end potential -0.4 V; step potential 0.005 V; modulation amplitude 0.025 V; sample volume: 5 µl; volume of measurement cell: 1000 µl (5 µl of sample; 995 µl acetate buffer). Time of accumulation was optimized.

2.6. Characterization of vaxi HA, HA-CdS and HA-CdTe complex by gel electrophoresis

Sodium dodecyl sulphate polyacrylamide gel electrophoresis (SDS-PAGE) was performed using Mini Protean Tetra apparatus with gel dimension of 8.3 × 7.3 cm (Bio-Rad, USA). First 12.5% (*m/V*) running, then 5% (*m/V*) stacking gel was poured. The gel was prepared from 30% (*m/V*) acrylamide stock solution with 1 % (*m/V*) bisacrylamide. The polymerization of the running or stacking gels was performed at room temperature for 30 min. Prior to analysis the samples were mixed with reducing sample buffer in a 2:1 ratio. The samples were incubated at 93 °C for 3 min, and then the sample was loaded onto a gel. For determination of the molecular mass, the protein ladder "Precision plus protein standards" from Biorad was used. The electrophoresis was run at 150 V for 1 h at laboratory temperature (23 °C) (Power Basic, Biorad USA) in tris-glycine buffer (0.025 M Trizma-base, 0.19 M glycine and 3.5 mM SDS, pH = 8.3). Then the gels were stained Coomassie-blue. The procedure of rapid Coomassie-blue staining was adopted from *Wong et al.* [22].

2.7. Robotic pippeting station

Computer controlled automated pipetting station, *ep-Motion 5075* (Eppendorf, Germany) was used for automated sample handling prior to electrochemical analysis. Transfer was ensured by a robotic arm with pipetting adaptors (TS50, TS300) and a gripper for platform transport (TG-T), placed on A1 position. Tips were placed in positions A3 (ePtips 300) and A2 (ePtips 50). At position A4 Thermomixer was located. At position B1, module reservoir for washing solutions and waste were placed. Position C1 was thermostated (Epthermoadapter PCR96). A thermorack for 24 x 1.5–2 ml microtubes (Position B3) was used to store working solutions. For sample preparation 96-well PCR plate with a maximal well volume of 200 μl was used. After separation, the magnetic particles were forced apart using a Promega magnetic pad (Promega, USA). The program sequence was edited and the station was controlled in pEditor 4.0 (Eppendorf).

2.8. Isolation of HA-QDs complexes by glycan modified paramagnetic particles

Streptavidin Dynabeads M-270 were purchased from Life Technologies (Carlsbad, California, USA). Biotinylated multivalent-glycan (01-078 [Neu5Acα2-3Galβ1-3GlcNAcβ1-PAA-biotin]) was supplied from GlycoTech (Gaithersburg, MD, USA). Vaxigrip® (HA) was purchased from Sanofi Pasteur (France). As the standard of HA, recombinant HA from H3N2 Influenza-A Virus Brisbane 10/07 (Prospecbio, Israel) was used. The first step of isolation was the pipetting of 10 μl of streptavidin Dynabeads M-270 to microplates PCR 96 (Eppendorf, Germany), and then the plate was transferred to a magnet. Stored solution was aspirated from the MPs and MPs were washed three times with 100 μl of phosphate buffer (0.3 M, pH 7.4, made from NaH_2PO_4 and Na_2HPO_4). Thereafter 20 μl of biotinylated glycan were added to each of the wells and incubated (30 min, 25 °C, 400 rpm). After incubation, the sample was washed three times with phosphate buffer (0.3 M, pH 7.4). Subsequently 20 μl of HA-QDs was added. Mixture in each well was further incubated (400 rpm) and washed three-times with 100 μl of phosphate buffer (0.3 M, pH 7.4). In the last step, 35 μl of phosphate buffer (0.3

M, pH 7.4) was added followed by the treatment of ultrasound needle (2 min). The plate was transferred to the magnet and the supernatant was analysed using AdT DPV Brdicka raction and DPASV. The effects of time and temperature of glycan HA-QDs complex interaction on the yield of product of isolation were investigated. The detected substances were identified as cadmium (QDs) and influenza antigen (HA from Vaxigrip).

2.9. Electrochemical analysis of the isolated sample

Two different methods of DPV were used for electrochemical detection of isolated complex. For HA determination optimized AdT DPV Brdicka reaction was used. Determination of metal part of HA-QDs complexes were performed by the optimized DPASV in the presence of acetate buffer. All of measurements were performed with a 663 VA Stand instrument (Metrohm, Switzerland).

2.10. Descriptive statistics

Data were processed using MICROSOFT EXCELs (USA) and STATISTICA.CZ Version 8.0 (Czech Republic). The results are expressed as mean ± SD unless noted otherwise. The detection limits (3 signal/noise, S/N) were calculated according to Long and Winefordner [23], whereas N was expressed as a standard deviation of noise determined in the signal domain unless stated otherwise.

3. RESULTS AND DISCUSSION

Recent reports showed that influenza can spread and undergo mutational changes more and more rapidly [24,25] and due to this fact causes illness among humans, or animal-human transmitted zoonosis. Highly pathogenic avian influenza (HPAI) is contagious viral disease affecting poultry with socio-economic impact. It is listed as a notifiable disease by the World Organisation for Animal Health (OIE) and represents a zoonotic threat [24]. The zoonotic outbreak of H7N9 subtype of HPAI that occurred in eastern China in the spring of 2013 resulted in 135 confirmed human cases, of which 44 were lethal [26]. Due to this fact early detection of this virus is highly needed [27]. The detection of the influenza virus is based on a wide range of techniques. Sauter and co-workers described X-ray crystal structures for several complexes between influenza virus hemagglutinin and derivatives of its cell-surface receptor, sialic acid (Neu5Ac) [28]. Gao and co-workers developed a panel with lysates of seasonal influenza virus (H1N1, H3N2 and B), serials of diluted H5N1 virus lysates, and *in vitro* transcribed H5 hemagglutinin (HA) and an artificial gene RNAs for real-time polymerase chain reaction (RT-PCR) and rRT-PCR quality control assessment [29]. However, these techniques required quite sophisticated equipment. In comparison, the electrochemical detection offers simple, attractive and easy-to-miniaturise alternative [30,31]. Here, we suggested a biosensor, which consists of HA-QDs complex isolation and subsequent electrochemical detection of target molecules [32-37]. In this

case, method for isolation and detection of HA labelled by two different QDs (CdS and CdTe) was designed and implemented.

3.1. Characterization of vaxi HA, CdTe and CdS, HA-CdS and HA-CdTe complex by electrochemical analysis

For indirect detection of HA and its signal amplification quantum dots was used as a marker. Two different QDs (CdTe and CdS) were applied and their effect on the isolation process was suggested. Quantum dots (QDs) own many unique optic properties such as high quantum yield, broad absorption spectra, narrow emission spectra, low bleaching and excellent photostability, and for this reason they are widely applied in biomedical imaging. Firstly, both of QDs and its complexes with HA from Vaxigrip ® were prepared by processes, which were described in Experimental section. Then individual substances: HA (Vaxigrip®) and Cd (CdTe and CdS) and the same substances in complexes (HA-CdTe and HA-CdS) were characterized by voltammetry.

3.1.1. Characterization of hemagglutinin by AdT DPV

For characterization of HA itself and HA in complexes with QDs, AdT DPV Brdicka reaction electrolyte was used. The main principle of AdT technique is based on an accumulation of target molecules onto the electrode surface from low volume and transfer of an electrode with adsorbed target molecules to the pure supporting electrolyte, where no interferences is present [38]. AdT DPV Brdicka reaction was utilized for detection of HA-QDs complex previously [39,40]. The reaction mechanism is based on the catalytic evolution of hydrogen on mercury electrode from protein containing SH groups in Brdicka solution. Typical voltammograms of HA and HA in complexes were compared in the Figs. 1A and 1B. Four peaks (X, Y, RS2Co, and Cat2 [41]) were detected and characterized in the obtained voltammograms. We were interested in two peaks that appeared only in HA-QDs complexes: peak X and peak Y. Peak Y was observed in both of complexes (HA-CdS and HA-CdTe) in same position (-1.09 ± 0.02 V). The difference was determined in position of peak X. In HA-CdS voltammogram peak X was detected at potential -0.99 ± 0.02 V. In HA-CdTe complex peak X was found at slightly negative potential (-1.05 ± 0.02 V). Our next interest was focused on peak Cat2 corresponding to the presence of –SH moieties, and interaction of HA with QDs by SH moieties in HA structure. During the interaction between HA and QDs, free -SH groups in HA are probably saturated by QDs and this effect causes occurrence of the peaks X and Y as a proof of metal reduction in HA-QDs complexes [42]. For this reason Cat2 peak of HA voltammogram was higher compared to HA-QDs complexes.
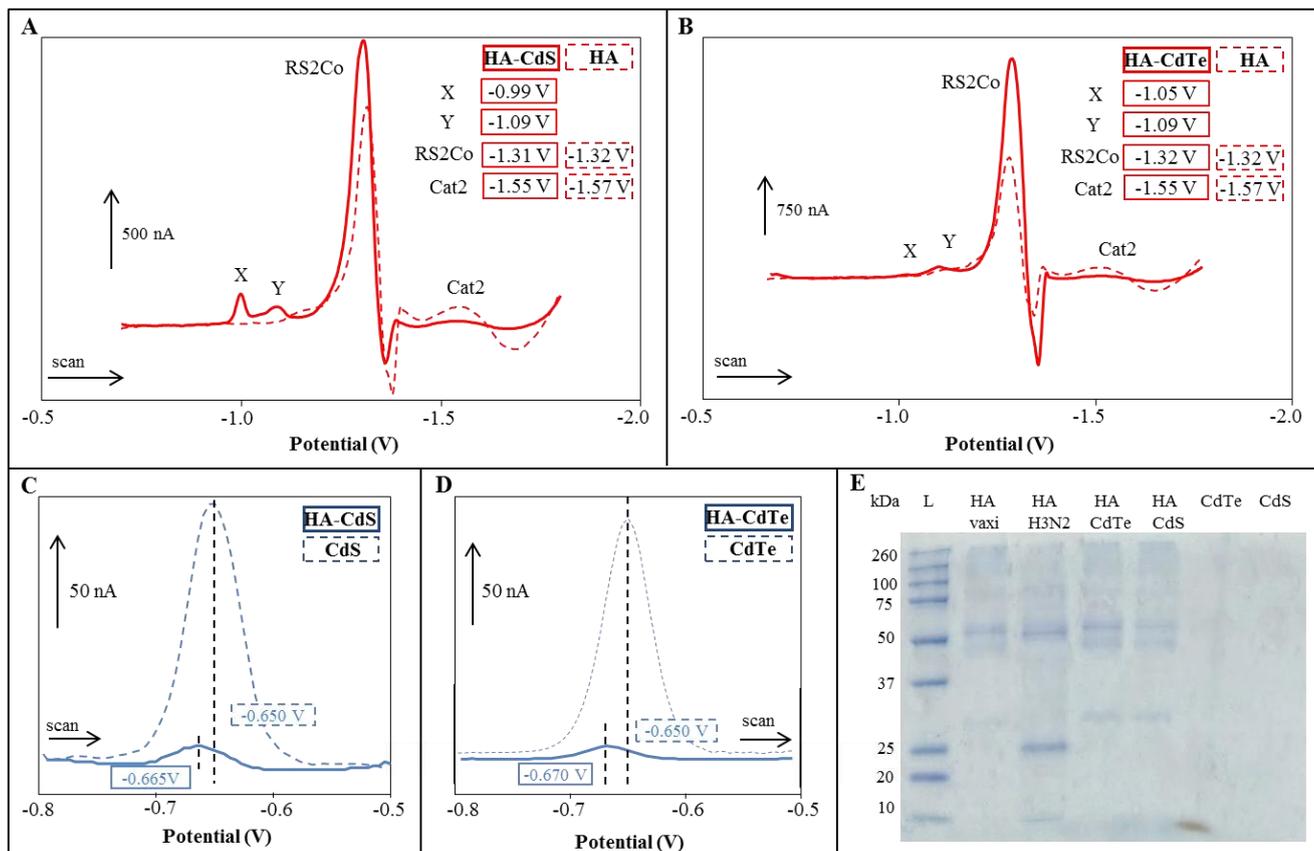
Figure 1. Comparison of typical DP voltammograms of HA in HA-QDs complex (solid line) and vaxi HA itself (dashed line) measured by AdT DPV Brdicka reaction for (**A**) HA-CdS and (**B**) HA-CdTe. For all measurements AdT DPV was used with parameters as follows: purge time 30 s, initial potential -0.7 V; end potential -1.8 V; accumulation time 120 s; potential step; 0.002 V; amplitude 0.025 V. Comparison of typical DP voltammograms of Cd in HA-QDs complex (solid line) and QDs itself (dashed line) measured by DPASV for (**C**) HA-CdS and (**D**) HA-CdTe. For Cd peak determination DPASV was used with parameters as follows: initial potential -0.8 V; end potential -0.5 V; deposition potential -0.8 V; equilibration time 5 s; modulation time 0.06 s; time interval 0.2 s; potential step 0.002 V; modulation amplitude 0.025 V. (**E**) Characterization of vaxi HA, HA standard (H3N2), HA-CdTe and HA-CdS complexes, CdTe and CdS quantum dots by SDS-PAGE. Reducing conditions and 10% gel were used.

3.1.2. Detection of cadmium by DPASV

The interaction of QDs with HA was also monitored electrochemically by DPASV in acetate buffer. Our interest was put on Cd peak. Its height and position were detected and differences between Cd peaks (in QDs and HA-QDs) were also described. Differences in position and peak height were described in Figs. 1C and 1D. Cd peak in both QDs is higher and peak potential is more positive compared to Cd peak in HA-QDs complexes. Cd peak position of both QDs is placed at potential -0.650 ± 0.005 V, Cd peak of HA-CdS at potential - 0.665 ± 0.005 V and Cd peak of HA-CdTe at potential -0.670 ± 0.005 V.

3.2. Characterization of vaxi HA, HA-CdS and HA-CdTe complex by gel electrophoresis

SDS-PAGE was used for characterization of HA (Vaxigrip ® and H3N2 standard), QDs (CdTe and CdS) and its complexes (HA-CdTe and HA-CdS) as it is shown in Fig. 1E. After Coomassie-blue staining of a gel, there are three bands of the different size corresponding to entire HA, HA1 and HA2 subunits in standard of H3N2. The entire HA (HA 0) protein is band with a molecular weight of 75 kDa, two others bands (approx. 50 kDa and 25kDa) corresponded to HA1and HA2 subunits. Compared to Vaxigrip ® HA itself and in complexes with CdTe and CdS QDs, the intensity of bands is lower and position of bands is little shifted. Shift is somewhat larger when we compared H3N2 standard with complexes than comparison with HA Vaxigrip ® itself. In lines of pure QDs there are no bands corresponded to HA.

3.3. Time of accumulation and calibration curves

After that we characterized that we successfully formed HA-QDs complex, we tested the effect of time of accumulation on HA and Cd peak heights of the formed complexes. The influence of time of accumulation on Cd peak in HA-CdS and HA-CdTe complexes is shown in Fig. 2A. In spite of the fact that the peak height was increasing in the whole tested interval, we selected 400 s as the compromise between sensitivity and the time of the analysis. Further, we tested the same parameter for HA detection b AdT DPV Brdcika reaction. Based on the results showed in Fig. 2B it follows that time of accumulation of 120 s was the optimal. Under the optimized parameters, we measured for Cd and HA and both types of QDs calibration curves, which are shown in Figs. 2C and 2D, respectively. All measured dependences were linear within tested concentration interval.

3.4. Optimization of HA-QDs complexes isolation and electrochemical analysis of isolated samples

Other authors described HA-glycan interaction as a basic specific connection for influenza virus isolation [43,44]. Comparison of binding of HA to the host cells and construction of biosensors is shown in Fig. 3A. Inspiration of natural targeting of influenza virus is obvious. Isolation of both of HA-QDs complexes were provided by the protocol, described in section 2.8 and according scheme presented in Fig. 3B. Streptavidin modified MPs were used as the platform, to which biotinylated glycan was bounded (Fig. 3B part a). Paramagnetic beads applications require setting particle properties (magnetic behaviour of the beads must be associated with appropriate bead surface modifications in order to allow covalent bonding or simple unspecific adsorption of biomolecules (proteins, antibodies, nucleic acids). Usually, the magnetic beads are tailor made for a specific final application [17]. In the next step there was HA-CdTe and/or HA-CdS complex bounded on the glycan conjugated MPs based on glycan-HA affinity (Fig. 3B part b). Fully automated setup was developed using an automatic pipetting robot as was described in section 2.7. The isolation products were analysed using electrochemical methods (Fig. 3B part c).
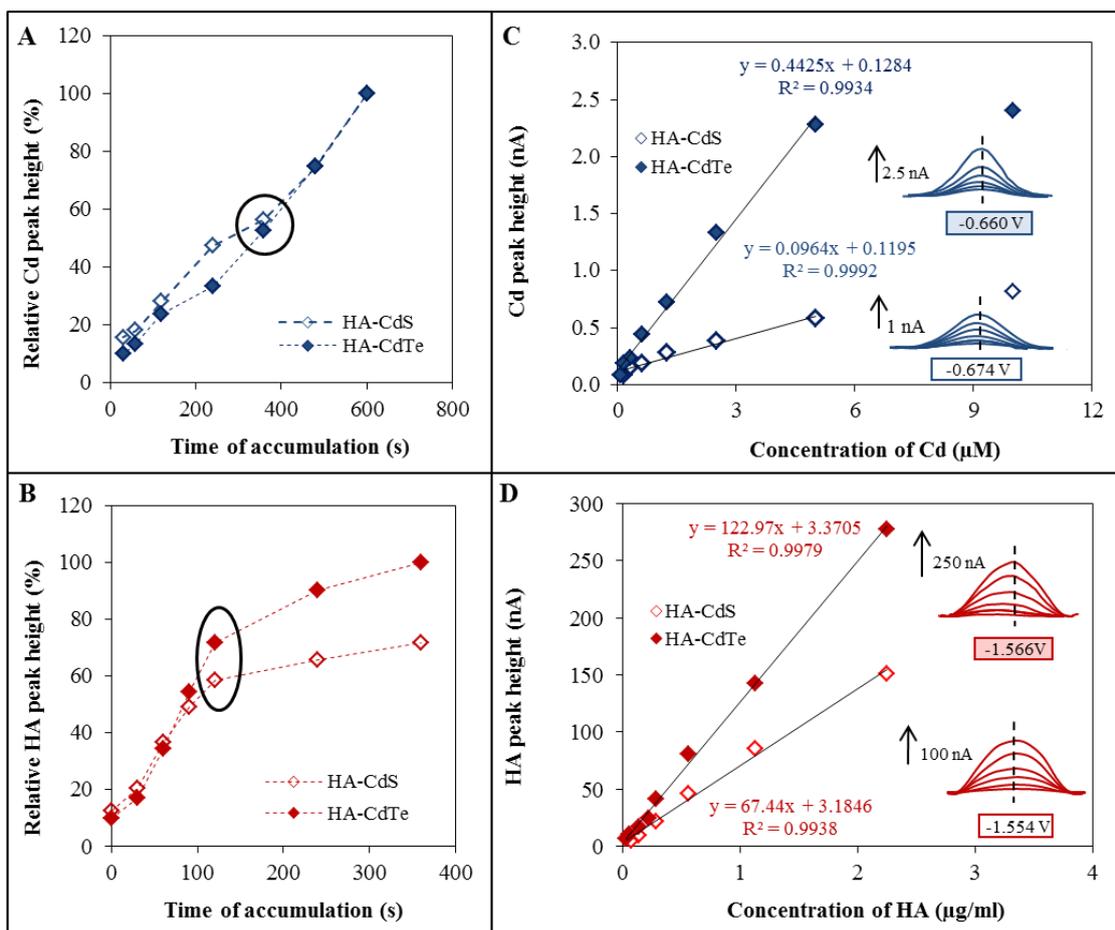
Figure 2. Dependence of relative peak height (related to the maximal value) on time of accumulation for (**A**) Cd peak and (**B**) HA peak. Dependence of relative peak height (related to the maximal value) on concentration of (**C**) cadmium and (**D**) concentration of HA. Red colour was used for HA (HA peak, measured by AdT DPV Brdicka reaction), blue colour was used for Cd (Cd peak, measured by DPASV). Unfilled points (HA-CdS complex), filled points (HA-CdTe complex).

The influence of time and temperature on the interaction between glycan and HA-QDs complex and on the yield of the isolated HA labelled by QDs was investigated. We tested six different values of temperatures (5, 25, 35, 45, 55, and 65 °C). Changes in Cd and HA peak heights showed increasing dependency related on the increasing temperature, but only to 45°C. Temperature of 45°C was established as the best according to the Cd peak height (Fig. 4A) and HA peak height (Fig. 4B).

Further, seven different times of reaction (5, 10, 15, 20, 30, 45 and 60 minutes) and its effect on Cd and HA peaks heights were investigated. The highest effect of reaction time was observed for Cd peak (Fig. 4C) after 20 minutes interaction for both quantum dots. Then the highest effect of reaction time was observed for HA peak (Fig. 4D). As the optimum 30 minutes (HA-CdS) was established, and for isolation of HA-CdTe time of interaction of 20 minutes was selected. If we summarize the results of the optimization, the best conditions were as follows: the reaction temperature 45 °C and the reaction time 20-30 minutes.
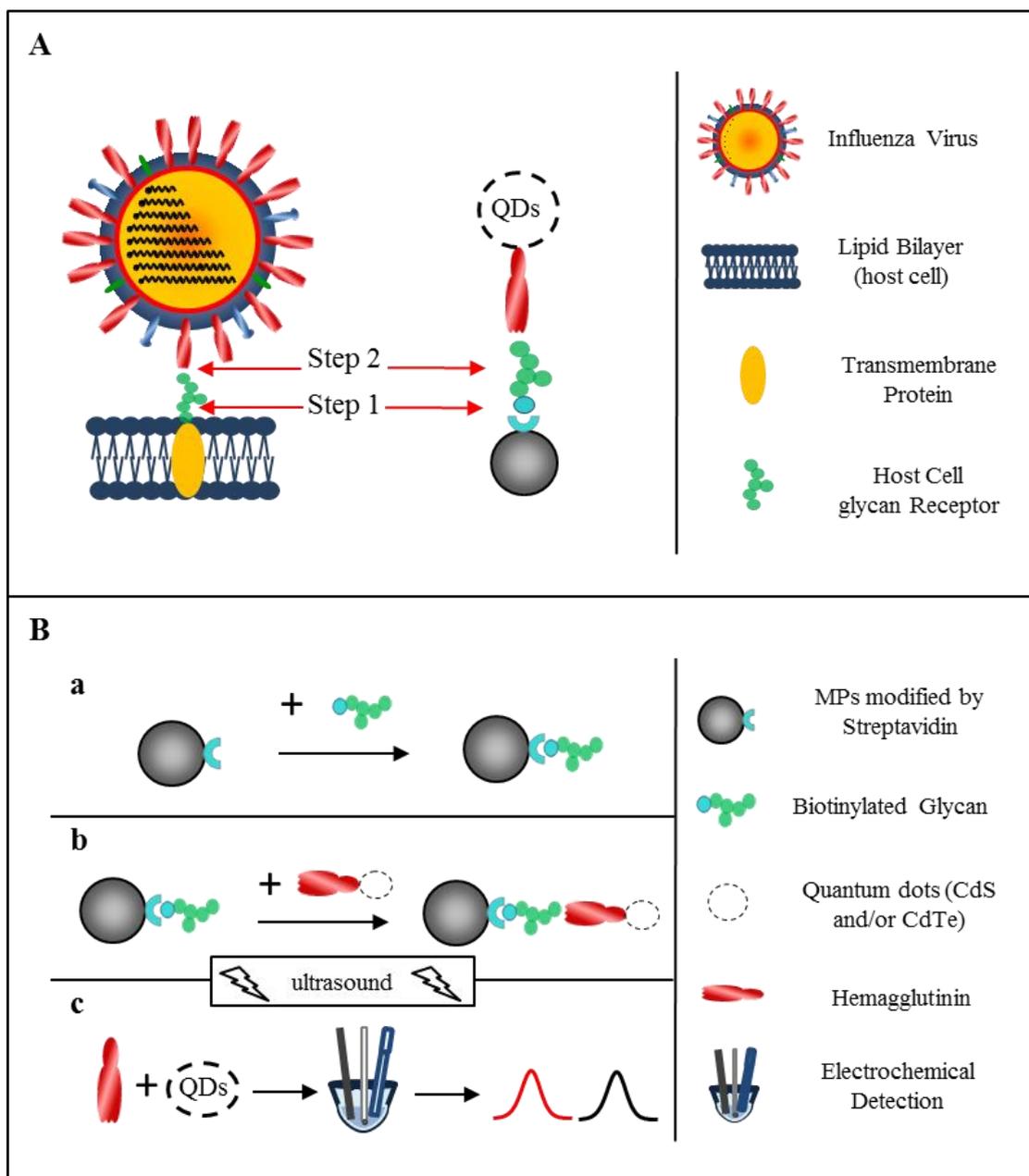
Figure 3. (**A**) Comparison of natural binding of influenza virus to glycan receptor located on the host cell and relation to our isolation procedure. (**B**) Scheme of fully automated isolation procedure connected with electrochemical detection of HA-QDs complexes. (**a**) Biotinylated glycan binding to streptavidin modified paramagnetic particles (MPs), (**b**) HA-QDs complex binding to glycan conjugated MPs, isolation of HA-CdS and/or HA-CdTe followed by ultrasound breaking of MPs-HA-QDs complexes, (**c**) electrochemical detection of HA and Cd peaks for both HA-QDs complexes by voltammetry. HA peak was measured by differential pulse voltammetry Brdicka reaction coupled with adsorptive transfer technique (AdT DPV) and Cd peak was measured by differential pulse anodic stripping voltammetry (DPASV).
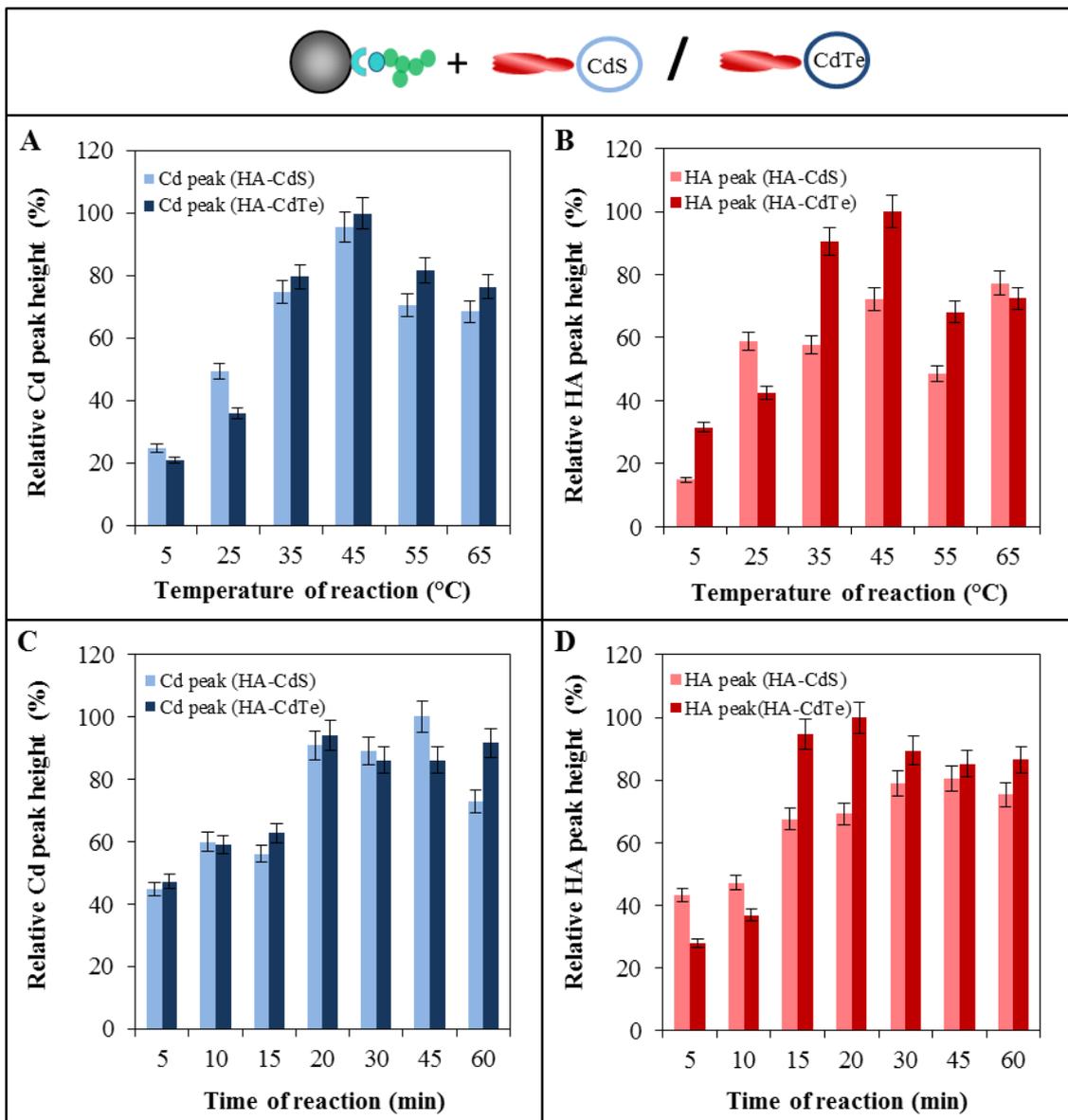
Figure 4. Effect of (**A**) and (**B**) temperature, and (**C**) and (**D**) reaction time on interaction between HA-QDs complex and MPs modified by glycan. The efficiency was observed by using electrochemical analysis of Cd peak for (**A**) temperature and (**C**) reaction time. All measurements of Cd peak were provided by DPASV. The second determined parameter was HA peak height and its affecting by (**B**) temperature (**D**) and reaction time. For all measurements of HA peak AdT DPV Brdicka reaction was used. Red colour was used for hemagglutinin, blue colour was used for cadmium. Light shade of individual colour was related to the HA-CdS complex, dark shade of individual colour was related to the HA-CdTe complex.

4. CONCLUSIONS

In this study we described method for rapid isolation of influenza HA, which was connected with electrochemical detection of HA labelled with various quantum dots (CdS and CdTe). The whole system was extended by automation of whole isolation protocol. An advantage of this assay is the

ability to provide dual electrochemical detection of products of the isolation as HA or metal part of the complex. The electrochemical detection of metal part of HA-QDs complexes could be more sensitive and suggested method can be considered as a suitable tool for determination of the specific influenza antigen. This method is not applicable only for the antigen of influenza virus but it can be extended for detection of specific proteins of other pathogens or cancer markers [45-50].

CONFLICT OF INTEREST:
The authors have declared no conflict of interest.

References

1. C.-M. Liao and S.-H. You, *Stoch. Environ. Res. Risk Assess.*, 28 (2014) 189.
2. T. N. Athmaram, S. Saraswat, B. Sikarwar, S. K. Verma, A. K. Singh and M. Boopathi, *J. Med. Virol.*, 86 (2014) 363.
3. J. P. Radomski, P. Plonski and W. Zagorski-Ostoja, *Mol. Phylogenet. Evol.*, 70 (2014) 29.
4. I.-B. Lian, H.-D. I. Wu, W.-T. Chang and D.-Y. Chao, *Plos One*, 9 (2014) 1.
5. L. Stone, R. Olinky and A. Huppert, *Nature*, 446 (2007) 533.
6. Q. J. Chen, S. P. Huang, J. J. Chen, S. Q. Zhang and Z. Chen, *PLoS One*, 8 (2013) 1.
7. Y. Abed, A. Pizzorno, X. Bouhy, C. Rheaume and G. Boivin, *J. Virol.*, 88 (2014) 1652.
8. K. Ohishi, *Aquabiology*, 28 (2006) 420.
9. T. W. Vahlenkamp and T. C. Harder, *Berliner Munchener Tierarztl. Wochenschr.*, 119 (2006) 123.
10. J. C. Jones, T. Baranovich, B. M. Marathe, A. F. Danner, J. P. Seiler, J. Franks, E. A. Govorkova, S. Krauss and R. G. Webster, *J. Virol.*, 88 (2014) 1175.
11. M. Imai, S. Herfst, E. M. Sorrell, E. J. A. Schrauwen, M. Linster, M. De Graaf, R. A. M. Fouchier and Y. Kawaoka, *Virus Res.*, 178 (2013) 15.
12. A. Gagnon, M. S. Miller, S. A. Hallman, R. Bourbeau, D. A. Herring, D. J. D. Earn and J. Madrenas, *PLoS One*, 8 (2013) 1.
13. E. Tognotti, *Emerg. Infect. Dis.*, 19 (2013) 254.
14. D. Kobasa, A. Takada, K. Shinya, M. Hatta, P. Halfmann, S. Theriault, H. Suzuki, H. Nishimura, K. Mitamura, N. Sugaya, T. Usui, T. Murata, Y. Maeda, S. Watanabe, M. Suresh, T. Suzuki, Y. Suzuki, H. Feldmann and Y. Kawaoka, *Nature*, 431 (2004) 703.
15. N. Komadina, J. McVernon, R. Hall and K. Leder, *Emerg. Infect. Dis.*, 20 (2014) 6.
16. B. Brandenburg, W. Koudstaal, J. Goudsmit, V. Klaren, C. Tang, M. V. Bujny, H. Korse, T. Kwaks, J. J. Otterstrom, J. Juraszek, A. M. van Oijen, R. Vogels and R. H. E. Friesen, *PLoS One*, 8 (2013) 1.
17. M. A. M. Gijs, *Microfluid. Nanofluid.*, 1 (2004) 22.
18. F. Gieseler, H. Gamperl, F. Theophil, I. Stenzel, T. Quecke, H. Ungefroren and H. Lehnert, *Cell Biol. Int.*, 38 (2014) 277.
19. L. P. Li, L. N. Xu, Z. Li, Y. Bai and H. W. Liu, *Anal. Bioanal. Chem.*, 406 (2014) 35.
20. H. Li, W. Y. Shih and W. H. Shih, *Ind. Eng. Chem. Res.*, 46 (2007) 2013.

21. J. L. Duan, L. X. Song and J. H. Zhan, *Nano Res.*, 2 (2009) 61.
22. C. Wong, S. Sridhara, J. C. A. Bardwell and U. Jakob, *Biotechniques*, 28 (2000) 426.
23. G. L. Long and J. D. Winefordner, *Anal. Chem.*, 55 (1983) A712.
24. S. Van Borm, M. Jonges, B. Lambrecht, G. Koch, P. Houdart and T. van den Berg, *Transbound. Emerg. Dis.*, 61 (2014) 86.
25. B. Bett, J. Henning, P. Abdu, I. Okike, J. Poole, J. Young, T. F. Randolph and B. D. Perry, *Transbound. Emerg. Dis.*, 61 (2014) 60.
26. J. D. Gabbard, D. Dlugolenski, D. Van Riel, N. Marshall, S. E. Galloway, E. W. Howerth, P. J. Campbell, C. Jones, S. Johnson, L. Byrd-Leotis, D. A. Steinhauer, T. Kuiken, S. M. Tompkins, R. Tripp, A. C. Lowen and J. Steel, *J. Virol.*, 88 (2014) 1502.
27. I. Grabowska, K. Malecka, A. Stachyra, A. Gora-Sochacka, A. Sirko, W. Zagorski-Ostoja, H. Radecka and J. Radecki, *Anal. Chem.*, 85 (2013) 10167.
28. N. K. Sauter, G. D. Glick, R. L. Crowther, S. J. Park, M. B. Eisen, J. J. Skehel, J. R. Knowles and D. C. Wiley, *Proc. Natl. Acad. Sci. U. S. A.*, 89 (1992) 324.
29. R. B. Gao, Y. Gao, L. Y. Wen, M. Shao, S. M. Zou, C. G. Li, L. Yang, X. Y. Li, W. Wang and Y. L. Shu, *BMC Infect. Dis.*, 11 (2011) 1.
30. M. Pedrero, S. Campuzano and J. M. Pingarron, *Sensors*, 9 (2009) 5503.
31. L. Krejcova, D. Hynek, V. Adam, J. Hubalek and R. Kizek, *Int. J. Electrochem. Sci.*, 7 (2012) 10779.
32. D. Fialova, L. Krejcova, L. Janu, I. Blazkova, O. Krystofova, D. Hynek, P. Kopel, J. Drbohlavova, M. Konecna, M. Vaculovicova, J. Kynicky, J. Hubalek, P. Babula, R. Kizek and V. Adam, *Int. J. Electrochem. Sci.*, 8 (2013) 10805.
33. L. Krejcova, D. Huska, D. Hynek, P. Kopel, V. Adam, J. Hubalek, L. Trnkova and R. Kizek, *Int. J. Electrochem. Sci.*, 8 (2013) 689.
34. L. Krejcova, D. Hynek, P. Kopel, M. A. R. Merlos, K. Tmejova, L. Trnkova, V. Adam, J. Hubalek and R. Kizek, *Int. J. Electrochem. Sci.*, 8 (2013) 4457.
35. L. Krejcova, L. Nejdl, D. Hynek, S. Krizkova, P. Kopel, V. Adam and R. Kizek, *Molecules*, 18 (2013) 15573.
36. L. Krejcova, L. Nejdl, M. A. Merlos Rodrigo, M. Zurek, M. Matousek, D. Hynek, O. Zitka, P. Kopel, V. Adam and R. Kizek, *Biosens. Bioelectron.*, 54 (2014) 421.
37. P. Sobrova, M. Vaculovicova, J. Hubalek, V. Adam and R. Kizek, *Int. J. Mol. Sci.*, 14 (2013) 13497.
38. P. Sobrova, M. Ryvolova, V. Pekarik, J. Hubalek, V. Adam and R. Kizek, *Int. J. Electrochem. Sci.*, 8 (2013) 12466.
39. V. Adam, J. Baloun, I. Fabrik, L. Trnkova and R. Kizek, *Sensors*, 8 (2008) 2293.
40. J. Petrlova, D. Potesil, R. Mikelova, O. Blastik, V. Adam, L. Trnkova, F. Jelen, R. Prusa, J. Kukacka and R. Kizek, *Electrochim. Acta*, 51 (2006) 5112.
41. P. Sobrova, L. Vyslouzilova, O. Stepankova, M. Ryvolova, J. Anyz, L. Trnkova, V. Adam, J. Hubalek and R. Kizek, *PLoS ONE*, 7 (2012) 1.
42. K. Tmejova, D. Hynek, P. Kopel, S. Krizkova, I. Blazkova, L. Trnkova, V. Adam and R. Kizek, *Colloid Surf. B-Biointerfaces* in press (2014).
43. E. Suenaga, H. Mizuno and K. K. R. Penmetcha, *Biosens. Bioelectron.*, 32 (2012) 195.
44. K. Hatano, K. Matsuoka and D. Terunuma, *Chem. Soc. Rev.*, 42 (2013) 4574.
45. J. Drbohlavova, V. Adam, R. Kizek and J. Hubalek, *Int. J. Mol. Sci.*, 10 (2009) 656.
46. M. Ryvolova, J. Chomoucka, L. Janu, J. Drbohlavova, V. Adam, J. Hubalek and R. Kizek, *Electrophoresis*, 32 (2011) 1619.
47. M. Ryvolova, K. Smerkova, J. Chomoucka, J. Hubalek, V. Adam and R. Kizek, *Electrophoresis*, 34 (2013) 801.
48. S. Skalickova, O. Zitka, L. Nejdl, S. Krizkova, J. Sochor, L. Janu, M. Ryvolova, D. Hynek, J. Zidkova, V. Zidek, V. Adam and R. Kizek, *Chromatographia*, 76 (2013) 345.

49. P. Sobrova, I. Blazkova, J. Chomoucka, J. Drbohlavova, M. Vaculovicova, P. Kopel, J. Hubalek, R. Kizek and V. Adam, *Prion*, 7 (2013) 349.
50. M. Stanisavljevic, L. Janu, K. Smerkova, S. Krizkova, N. Pizurova, M. Ryvolova, V. Adam, J. Hubalek and R. Kizek, *Chromatographia*, 76 (2013) 335.